Redox Biology 59 (2023) 102569

Contents lists available at ScienceDirect

Redox Biology

journal homepage: www.elsevier.com/locate/redox

Silica nanoparticles aggravated the metabolic associated fatty liver disease through disturbed amino acid and lipid metabolisms-mediated oxidative stress

Alimire Abulikemu [a,b,1], Xinying Zhao [b,c,1], Hailin Xu [b,c], Yan Li [a,b], Ru Ma [a,b], Qing Yao [b,c], Ji Wang [b,c], Zhiwei Sun [b,c], Yanbo Li [b,c,*], Caixia Guo [a,b,**]

[a] Department of Occupational Health and Environmental Health, School of Public Health, Capital Medical University, Beijing, 100069, China
[b] Beijing Key Laboratory of Environmental Toxicology, Capital Medical University, Beijing, 100069, China
[c] Department of Toxicology and Sanitary Chemistry, School of Public Health, Capital Medical University, Beijing, 100069, China

ARTICLE INFO

Keywords:
Silica nanoparticle
Hepatotoxicity
Metabolomics
Metabolic associated fatty liver disease
Oxidative stress

ABSTRACT

The metabolic associated fatty liver disease (MAFLD) is a public health challenge, leading to a global increase in chronic liver disease. The respiratory exposure of silica nanoparticles (SiNPs) has revealed to induce hepatotoxicity. However, its role in the pathogenesis and progression of MAFLD was severely under-studied. In this context, the hepatic impacts of SiNPs were investigated *in vivo* and *in vitro* through using ApoE$^{-/-}$ mice and free fatty acid (FFA)-treated L02 hepatocytes. Histopathological examinations and biochemical analysis showed SiNPs exposure *via* intratracheal instillation aggravated hepatic steatosis, lipid vacuolation, inflammatory infiltration and even collagen deposition in ApoE$^{-/-}$ mice, companied with increased hepatic ALT, AST and LDH levels. The enhanced fatty acid synthesis and inhibited fatty acid β-oxidation and lipid efflux may account for the increased hepatic TC/TG by SiNPs. Consistently, SiNPs induced lipid deposition and elevated TC in FFA-treated L02 cells. Further, the activation of hepatic oxidative stress was detected *in vivo* and *in vitro*, as evidenced by ROS accumulation, elevated MDA, declined GSH/GSSG and down-regulated Nrf2 signaling. Endoplasmic reticulum (ER) stress was also triggered in response to SiNPs-induced lipid accumulation, as reflecting by the remarkable ER expansion and increased BIP expression. More importantly, an UPLC-MS-based metabolomics analysis revealed that SiNPs disturbed the hepatic metabolic profile in ApoE$^{-/-}$ mice, prominently on amino acids and lipid metabolisms. In particular, the identified differential metabolites were strongly correlated to the activation of oxidative stress and ensuing hepatic TC/TG accumulation and liver injuries, contributing to the progression of liver diseases. Taken together, our study showed SiNPs promoted hepatic steatosis and liver damage, resulting in the aggravation of MAFLD progression. More importantly, the disturbed amino acids and lipid metabolisms-mediated oxidative stress was a key contributor to this phenomenon from a metabolic perspective.

1. Introduction

At present, the number of nano-products is growing rapidly. By 2024, the global nanotechnology market is expected to exceed $125 billion in accordance with a white paper published by the Springer Nature. However, the updated toxicological studies of nanomaterials (NMs) associated with their possible environmental and human health effects lag far behind the rapid rise in their application. Silica nanoparticles (SiNPs) as one of the most popular NMs, have been utilized in biomedical fields for drug carriers, gene therapy, diagnosis, and molecular imaging [1]. Along with these applications, their potential side effects on human health have got increasing attention. SiNPs can enter into the human body *via* inhalation, ingestion, skin contact, and even injection for medical applications [2]. It was commonly accepted inhalation as the most principal route of human exposure to SiNPs, particularly in occupational environment. There was evidence showed inhaled SiNPs induced inflammation and epithelial cell proliferation in lungs [3], and entered the circulatory system through the "blood-lung

* Corresponding author. Beijing Key Laboratory of Environmental Toxicology, Capital Medical University, No.10 Xitoutiao, You An Men, Beijing, 100069, China.
** Corresponding author. Beijing Key Laboratory of Environmental Toxicology, Capital Medical University, No.10 Xitoutiao, You An Men, Beijing, 100069, China.
E-mail addresses: ybli@ccmu.edu.cn (Y. Li), guocx@ccmu.edu.cn (C. Guo).
[1] The two authors contributed to this work equally.

https://doi.org/10.1016/j.redox.2022.102569
Received 17 November 2022; Accepted 2 December 2022
Available online 5 December 2022

barrier". It is well known that inhaled particles could be detected in extrapulmonary organs [4,5]. To date, numerous studies have revealed that SiNPs exposure led to harmful biological responses in diverse organs [6,7].

The liver is the largest solid organ in the body where most toxins are bio-transformed, and is also a major site for nanoparticles (NPs) accumulation regardless of exposed route [8,9]. A number of toxicological studies have indicated that SiNPs caused liver injury, including oxidative stress, DNA damage, inflammation, disturbance in metabolism [10–12], etc., probably contributing fibrosis and liver failure ultimately [13–15]. Currently, the nano-safety of susceptible populations is of great concern [7,16]. However, the interactions between SiNPs and biological systems under disease-state condition, and underlying mechanisms are poorly elucidated.

Metabolic associated fatty liver disease (MAFLD; previously named as non-alcoholic fatty liver disease) [17], is known as the most common cause of chronic liver disease in the world, which has a prevalence rate of 20%–40%, and up to 95% patients with metabolic comorbidities, such as hyperlipidemia, obesity and diabetes [18–20]. MAFLD is featured by the abnormal accumulated lipids and steatosis of liver parenchyma cells, and includes a board spectrum of liver diseases, *e.g.*, simple steatosis, fibrosis, cirrhosis and, ultimately, hepatocellular carcinoma [21,22], but their pathogenesis and progression still incompletely understood.

Metabolomics, a powerful technique to discover new biomarkers, is the qualitative and quantitative description of metabolic processes by nuclear magnetic resonance and mass spectrometry [23]. As a new branch of science after genomics and proteomics, metabolomics has been used to elucidate mechanisms of many diseases and explore potential biomarkers or therapeutic targets for clinical diagnosis and treatment [24,25]. Currently, the benefits of metabolomics have been gradually utilized in nanotoxicological research [10,26,27]. In addition, studies have reported that apolipoprotein E knockout ($ApoE^{-/-}$) mice fed by high-fat diet (HFD) model closely resembles the pathophysiology of progressive MAFLD in humans [28,29]. Also, the free fatty acid (FFA)-treated hepatocyte is an *in vitro* cell model for hepatic steatosis.

In this context, we investigated the impacts of SiNPs exposure on the improvement of MAFLD *via in vivo* and *in vitro* models, and in particular, performed metabolomic analysis using ultra-performance liquid chromatography-mass spectrometry (UPLC-MS) to reveal potential mechanisms.

2. Materials and methods

2.1. The characterization of SiNPs

The obtained SiNPs by Stöber method was characterized as previously described [30], including particle morphology observed under a JEM2100 transmission electron microscope (TEM; JEOL, Japan) and particle size distribution analyzed by using ImageJ software; zeta potential and hydrodynamic sizes in dispersion media measured by a Zetasizer Nano-ZS90 analyzer (Malvern, UK); purity and endotoxin determination using Agilent's inductively coupled plasma atomic emission spectrometer (Agilent 720, USA) and gel-clot limulus amebocyte lysate assay, separately.

2.2. In vivo experiments

2.2.1. Animal procedures

Male $ApoE^{-/-}$ mice (specific pathogen free, SPF) from Vital River Laboratory Animal Technology Co. Ltd (Beijing, China) were used for the *in vivo* experiments. All the mice were housed in sterilized filter-topped cages under conditions of controlled light (12 h light/dark cycle), temperature (24 ± 1 °C) and humidity (50 ± 5%) with free access to food and sterile water. At five weeks of age, all mice were switched to a HFD feeding containing 21% fat, 0.15% cholesterol and 34% sucrose until the experimental termination. After 4-w on the HFD, the mice were randomly divided into the following four groups: (1) low-dose SiNPs group (1.5 mg/kg·bw, n = 8), (2) middle-dose SiNPs group (3.0 mg/kg·bw, n = 9), (3) high-dose SiNPs group (6.0 mg/kg·bw, n = 9), and (4) control group (same volume of 0.9% saline, n = 9). SiNPs or vehicle was administered *via* intratracheal instillation, once per week for 12 times in total. In line with previous publishing [31,32], the dosage of SiNPs was set on the basis of the permissible concentration-time weighted average (PC-TWA) of amorphous silica dioxide (SiO_2), human respiratory parameters and equivalent dose conversion to mimic actual workplace exposure scenarios. In the experimental period, food intake and body weight were monitored and weighed every week. Four-week after the cessation of SiNPs treatment, mice were fasted overnight (8–10 h), then anesthetized and sampled. The liver tissues were rapidly harvested and weighted, with a portion for histopathological examination and others immediately frozen at −80 °C until subsequent analysis. All animal care and experimentation were conducted according to National Guidelines for Animal Care and Use, and approved by the Animal Experimental Ethics Committee of Capital Medical University (Ethical number, AEEI-2018-002).

2.2.2. Histopathological examination

The mice liver samples were immediately immersed in a 10% formalin solution for fixation, and then embedded in paraffin, sectioned into 5-μm slices, and placed on glass slides. Hematoxylin & eosin (HE) and Masson's trichrome were carried out to evaluate histopathological alterations in the liver. All slides were scanned using Pannoramic SCAN system (3DHISTECH, Hungary). Subsequently, the histopathology of each slide was observed, evaluated and scored by an investigator blinded for the experiment, and checked by a certified veterinary pathologist. Of note, the scoring criteria for MAFLD were based on the SAF method (S: steatosis, A: activity, S: fibrosis) [33].

2.2.3. Lipid assay

Oil Red O staining was applied for steatosis assessment. Moreover, the contents of total cholesterol (TC) and triglyceride (TG) in liver tissues (n = 8 per group) were analyzed using the corresponding commercial kit according to the manufacture's protocols (Nanjing Jiancheng, China).

2.2.4. Biochemical analysis

The activities of lactate dehydrogenase (LDH), alanine aminotransferase (ALT) and aspartate transaminase (AST) in liver tissues (n = 8 per group) were examined by using the commercial colorimetric assay kits (Nanjing Jiancheng, China).

2.2.5. Ultrastructure observation

The fresh liver tissues were cut into 1 mm^3 and immediately immersed in 2.5% glutaraldehyde for fixation. After three-time rinse with 0.1 M phosphate buffer, all the samples were postfixed with 4% osmium tetroxide. Then samples were rinsed, stained with uranyl acetate and lead citrate, dehydrated in a graded series of ethanol, and finally embedded them in epoxy resin. Random sections were cut (50 nm), collected on naked copper mesh grids, and viewed through a TEM (Hitachi HT7700; Hitachi, Japan).

2.2.6. UPLC-MS-based non-targeted metabolomics

Metabolic profiles of the liver tissues were acquired by UPLC-MS approach. The detailed procedure and corresponding analysis were all provided in Supplementary files, Supplementary Methods.

2.2.7. Oxidative stress determination

Hepatic reactive oxygen species (ROS) level was evaluated by incubating liver slides with DHE working liquid (1 mg/mL, 30 min; Sigma, USA) at room temperature in darkness. The nuclei were stained with DAPI (2 μg/mL, 10 min; Servicebio, China). Laterly, the slides were observed under a fluorescence microscope (Nikon Eclipse C1, Japan).

Ultimately, the fluorescence intensity was analyzed with Image J software, which was calibrated with the number of DAPI. Moreover, the hepatic ROS contents were quantitatively determined by using a commercial kit (Bestbio, China) in strictly accordance with the product's manual.

In addition, liver samples (n = 8 per group) were lysed with protein lysis buffer at a ratio of 1:9 (w/v). The supernatants were harvested for the determination of reduced glutathione (GSH), oxidized glutathione (GSSG) and malondialdehyde (MDA) with commercially available kits (Nanjing Jiancheng, China), in accordance with the manufacturer's instructions.

2.2.8. Immunohistochemical analysis

The expression of glucose-regulated protein 78 (GRP78), also known as immunoglobulin heavy chain binding protein (BIP) was detected by immunohistochemical staining through using its rabbit monoclonal antibody (CST, USA). Ultimately, sections (n = 3 per group) were observed by an optical microscope (Olympus, Japan).

2.3. In vitro experiments

2.3.1. Cell model

Normal human hepatic cell line (L02) from Nanjing Keygen Biotech cell library, China, were cultured in DMEM (Corning, USA) containing 10% fetal bovine serum (FBS; Thermo Fisher Scientific, USA) with 5% CO_2 at 37 °C. When cells were grown to about 60% confluency, 2 mM FFA (oleic acid/palmitic acid, 2:1 ratio, Sigma-Aldrich, USA) was added for a 24-h incubation to induce steatosis in hepatocytes [34], followed by another 24-h exposure to SiNPs (50 μg/mL). Furthermore, the dose of SiNPs exposure was based on one-half of IC_{50} in our previous study [35].

2.3.2. Intracellular lipid analysis

In accordance with previous description [32], Oil Red O staining was performed, and images were captured under an inverted optical microscope (Olympus IX81, Tokyo, Japan). The percentage of positive staining area to the total cell area was analyzed using Image J software. Moreover, the intracellular TC mass was quantified using a commercial kit (Applygen, China).

2.3.3. ROS assay

The intracellular ROS content was measured by 2′,7′-dichlorofluorescein diacetate (DCFH-DA; Beyotime, China) labeling according to previous literature [36]. Briefly, the cells were incubated with DCFH-DA working solution in the dark (10 mM, 37 °C, 30 min). Thereafter, the cells were rinsed by phosphate buffered saline (PBS), and the fluorescent intensity was detected using a NovoCyte flow cytometer (Agilent, USA).

2.4. Western blotting analysis

Expressions of BIP and C/EBP homologous protein (CHOP) proteins were detected by Western blot assay and standardized by GAPDH. The primary antibodies for BIP and CHOP were purchased from Proteintech, USA, whilst that for GAPDH from CST, USA. Lastly, the fluorescent signal was obtained by an Odyssey® CLx Imaging System (Gene Company Limited, Hong Kong), and analyzed using Image Studio™ software.

2.5. Quantitative real-time PCR

Total RNA was extracted from fresh frozen liver tissues (n = 4 per group) and *in vitro* cultured hepatocytes (n = 3) using a total RNA kit (TIANGEN, Beijing). An ultra-micro spectrophotometer (ThermoFisher, USA) was utilized to analyze the quantity of all RNA samples. As previously described [37], 2 μg of the extracted RNA was reverse-transcribed to cDNA, and the real-time PCR was performed. All experiments were conducted in triplicates. Using *β-actin* as an internal reference, the relative gene expression was ultimately calculated through fold induction ($2^{-\Delta\Delta ct}$). The sequences of primers used were detailed in Supplementary files, Table S1.

2.6. Statistical analysis

Metabolomics-related analysis methods have been described in Supplementary Methods. Data were showed as mean ± standard deviation (SD). Statistical significance in SAF Score was determined through Kruskal-Wallis followed by Nemenyi. For quantitative data, all the data conformed to the normal distribution (Shapiro-wilk method). Student's *t*-test was performed for two-group comparison, and one-way analysis of variance (ANOVA) was carried out for multiple comparison with Dunnett's T3 (heterogeneous data) or Dunnett (T) (homogeneous data) for post hoc test. Two-way ANOVA was used to analyze the interactions between SiNPs and FFA. And also, the relationship between the differential metabolites and liver-related diseases was referred by the Human Metabolome Database (https://hmdb.ca/). Pearson method was adopted for correlation analysis. Differences were considered statistically significant at bilateral $p < 0.05$.

3. Results

3.1. Characterization of SiNPs

As shown in Fig. 1, SiNPs had near-spherical shape, and dispersed with average diameter of 59.98 nm. Their hydrodynamic sizes and zeta potential in distilled water were present in Table 1. Besides, the synthesized SiNPs was free of endotoxin and had purity more than 99.9%.

3.2. SiNPs aggravated histopathological progression and dysfunction in the liver of HFD-fed ApoE$^{-/-}$ mice

As depicted in Fig. 2A, disorder in arrangement and hierarchy of liver cells, the degeneration and vacuolization of hepatocytes, and the infiltration of inflammatory cells in the liver, were clearly seen in SiNPs-treated groups in comparison with the control group. Oil Red O staining and corresponding semi-quantitative analysis manifested an increased lipid deposition upon SiNPs exposure (Fig. 2B and D). Even worse, SiNPs exposure induced an increased collagen deposition in hepatic tissue as reflected by Masson staining (Fig. 2C and E). A final evaluation of these histopathological alterations was done using SAF score analysis. See detail in Table 2.

As illustrated in Fig. 2F–H, significantly dose-dependent increase of

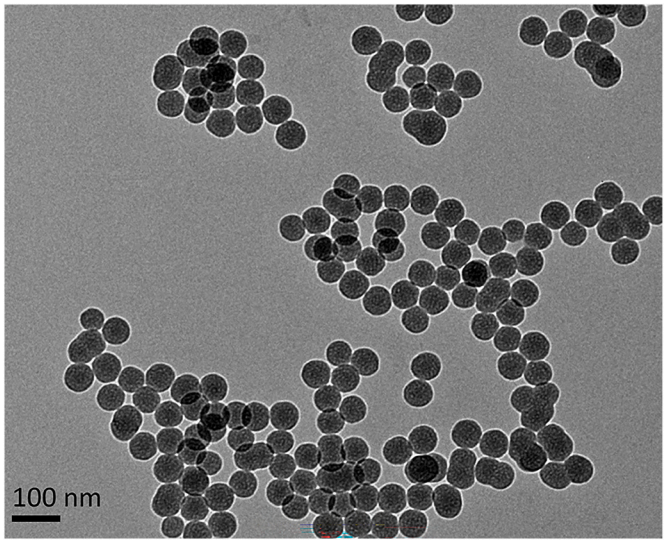

Fig. 1. Representative TEM image of tested SiNPs. Scale bar, 100 nm.

Table 1
Characterization of SiNPs.

Characteristic	SiNPs
Size and distribution, nm (mean ± standard deviation)	59.98 ± 5.71
Hydrodynamic size in water, nm (mean ± standard deviation)	96.23 ± 3.76
Zeta Potential (mV)	−36.40 ± 3.10
Morphology	Spheroid
Aggregation	Absent
Crystalline structure	Amorphous
Purity (%)	99.99
Endotoxin	Negative

Abbreviation: SiNPs, silica nanoparticles.

hepatic LDH, ALT and AST activities, the major parameters to reflect liver function, were detected in SiNPs-exposed livers of mice. In line with the Oil Red O staining, SiNPs led to a significant increase of hepatic TC and TG levels (Fig. 2I and J). PCR analysis showed that in comparison to the control, SiNPs significantly up-regulated the mRNA levels of genes related to fatty acid synthesis (i.e., *Fasn*, *Elovl6* and *Scd1*), conversely, down-regulated those involved in fatty acid beta-oxidation (*Cpt1a*, *Acox1* and *Pparα*) and lipid efflux (*Scarb1*, *Abca1*, *Abcg1* and *Lxrα*; Fig. 2K). The noticed increase of the transcriptional levels of *Cpt1a* and *Acox1* in low- or medium-dose group may represent negative feedback in response to SiNPs-triggered lipid deposition in the liver. In addition, SiNPs had no influence on body weight, weight gain and the coefficient of liver (Supplementary files, Table S2).

3.3. SiNPs activated oxidative stress, endoplasmic reticulum (ER) stress, and promoted lipid deposition in FFA-treated hepatocytes

Lipid accumulation had noticeably increased in the L02 cells after

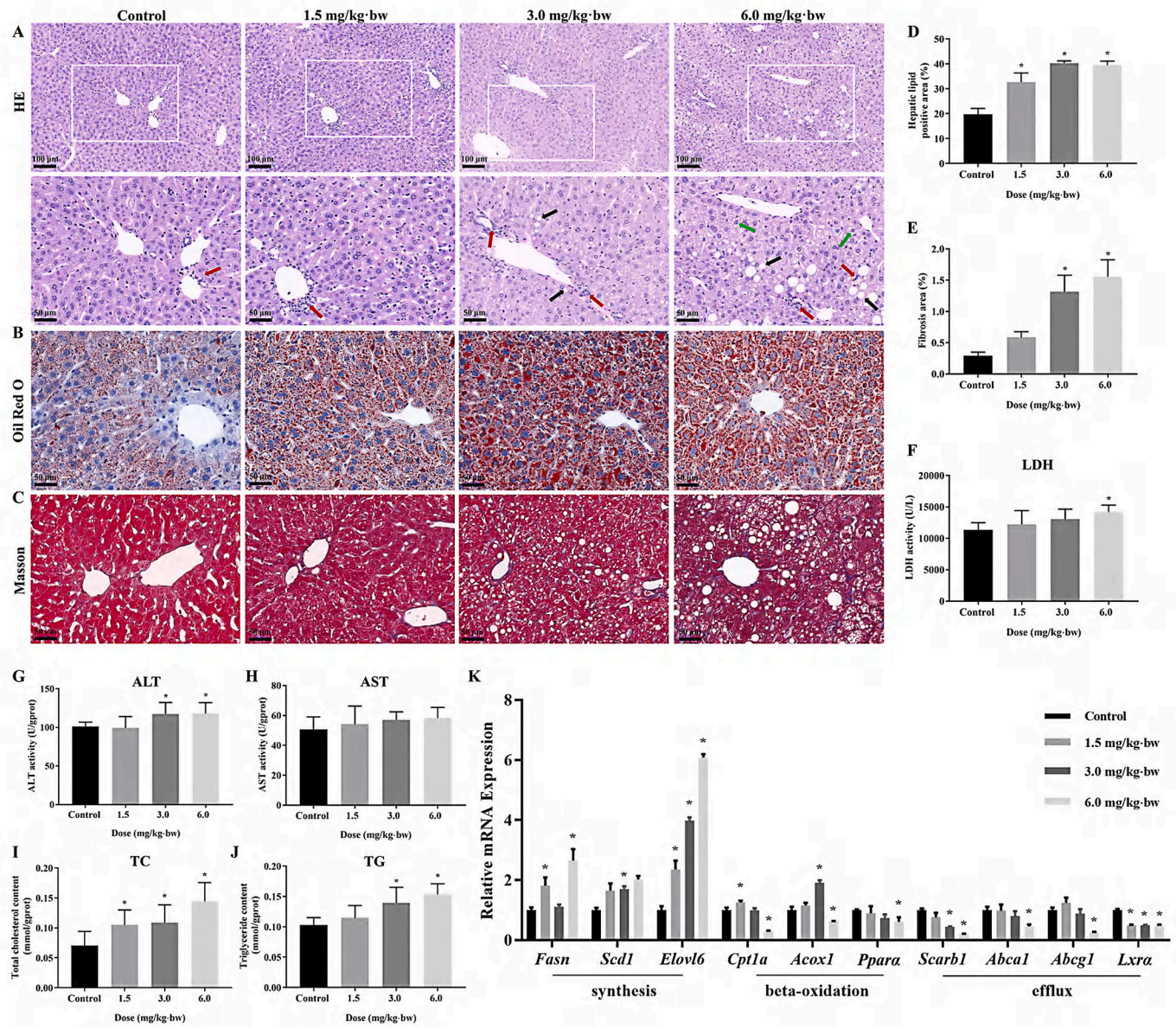

Fig. 2. Histopathological alterations, injury and lipid accumulation caused by SiNPs in the liver. (A) Representative HE-stained images of liver tissues (n = 3 per group). Fat vacuoles of different sizes (black arrow). Inflammatory cell infiltration (red arrow). The Mallory bodies (green arrow). Oil Red O (B) and Masson's trichrome staining (C) of liver tissues and corresponding semi-quantifications (D - E; n = 3 per group). Increased LDH (F), ALT (G) and AST (H) were detected in SiNPs-treated liver (n = 8 per group). Moreover, the determination of TC (I) and TG (J) level in the liver (n = 8 per group) indicated advanced steatosis caused by SiNPs. (K) Relative expression of genes related to lipid metabolism (n = 4 per group). The scale bar, 100 or 50 μm. Data are shown as mean ± SD. *$p < 0.05$ *vs* control. (For interpretation of the references to color in this figure legend, the reader is referred to the Web version of this article.)

Table 2
The SAF score in mice with metabolic associated fatty liver disease (MAFLD)

Group	Steatosis Score	Activity Score	Fibrosis Score	SAF Score	*p*
Control	0.33 ± 0.52	0.17 ± 0.41	1.17 ± 0.41	1.67 ± 0.52	< 0.001
1.5 mg/kg·bw	0.83 ± 0.75	0.67 ± 0.82	2.33 ± 0.52	3.83 ± 0.98	
3.0 mg/kg·bw	1.67 ± 1.21	2.17 ± 0.98	2.83 ± 0.41*	6.67 ± 2.07*	
6.0 mg/kg·bw	3.00 ± 1.26*	3.17 ± 0.75*	3.50 ± 0.55*	9.67 ± 1.86*	

Data are expressed as the means ± SD, *$p < 0.05$ *vs* control. Statistical significance is determined through Kruskal-Wallis followed by Nemenyi.

FFA treatment, and further remarkably increased upon SiNPs stimuli, as evidenced by the lipid droplets staining by Oil Red O (Fig. 3A and B), and the intracellular TC determination (Fig. 3D). That could be well demonstrated by the interaction assessment between SiNPs and FFA using two-way ANOVA (Fig. 3C and E). Moreover, compared with FFA treatment group, SiNPs could greatly increase the intracellular ROS level (Fig. 3F and G), and up-regulated the protein levels of BIP and CHOP (Fig. 3H).

3.4. SiNPs triggered oxidative stress and ER stress in the liver of HFD-fed $ApoE^{-/-}$ mice

As shown in Fig. 4A and B, an enhanced ROS level was clearly seen in SiNPs-treated liver tissues when compared to the control. Consistently, a dose-dependent increase in hepatic ROS accumulation was manifested in Fig. 4C. Moreover, the SiNPs-exposed livers exhibited a dose-dependent decrease in GSH content (Fig. 4D) and the ratio of GSH to GSSG (Fig. 4F), whilst elevation in GSSG (Fig. 4E) and MDA level (Fig. 4G). Interesting, the elevated ALT content in liver tissue showed negative correlation with the ratio of GSH to GSSG (Fig. 4H), and positive correlation with the ROS content (Fig. 4I). Besides, RT-PCR results

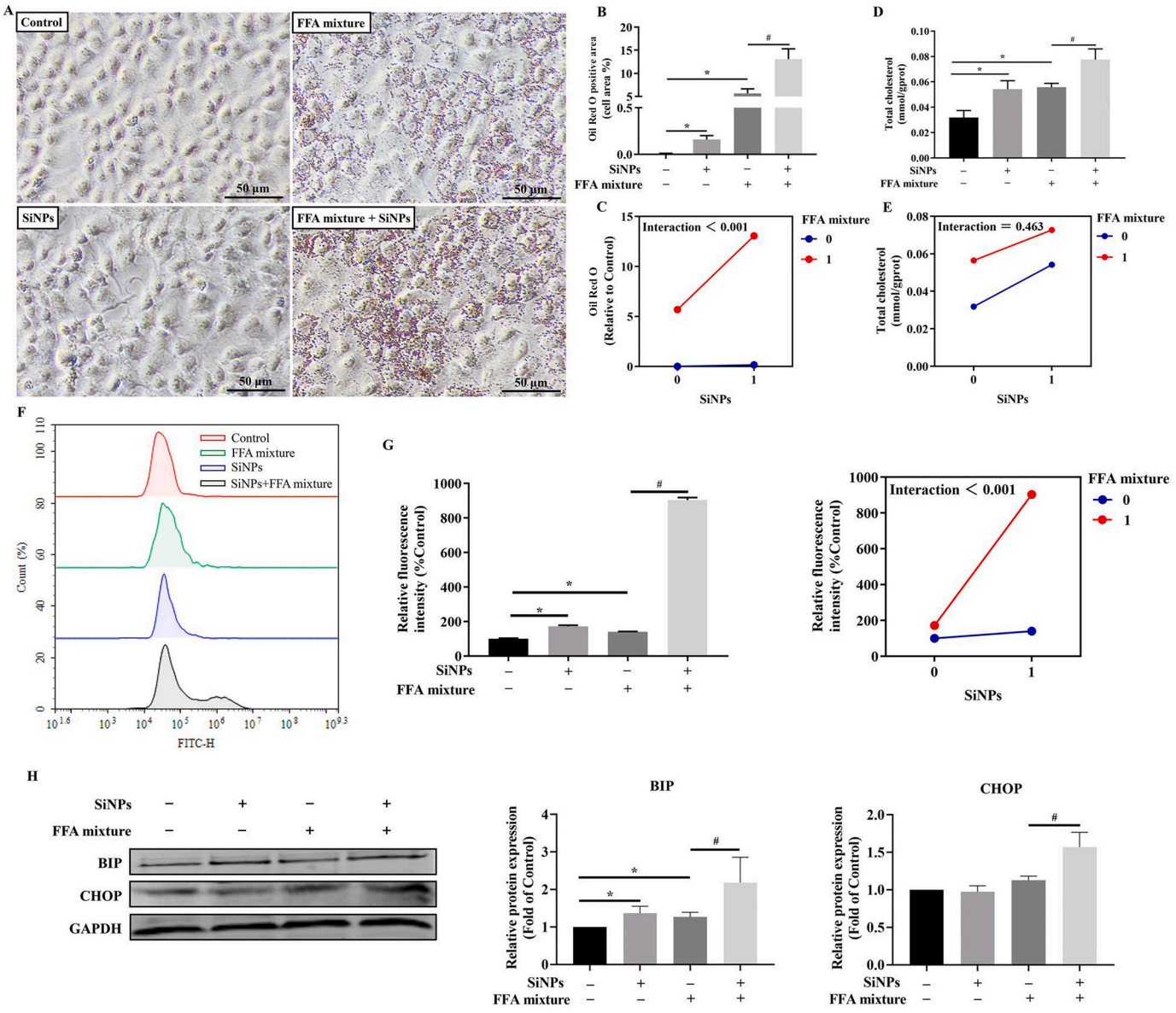

Fig. 3. Lipid accumulation, oxidative stress and ER stress in MAFLD cell model. Oil Red O staining (A) and corresponding semi-quantitative analysis (B), the determination of TC level (D) in L02 cells, and the interaction analysis (C and E) indicated advanced steatosis caused by SiNPs. ROS content measurement (F) and the interaction analysis (G) were shown, as well as the protein expressions of BIP and CHOP (H). The scale bar, 50 μm. Data are shown as mean ± SD, n = 3. *$p < 0.05$ *vs* control and $^{\#}p < 0.05$ *vs* FFA mixture. (For interpretation of the references to color in this figure legend, the reader is referred to the Web version of this article.)

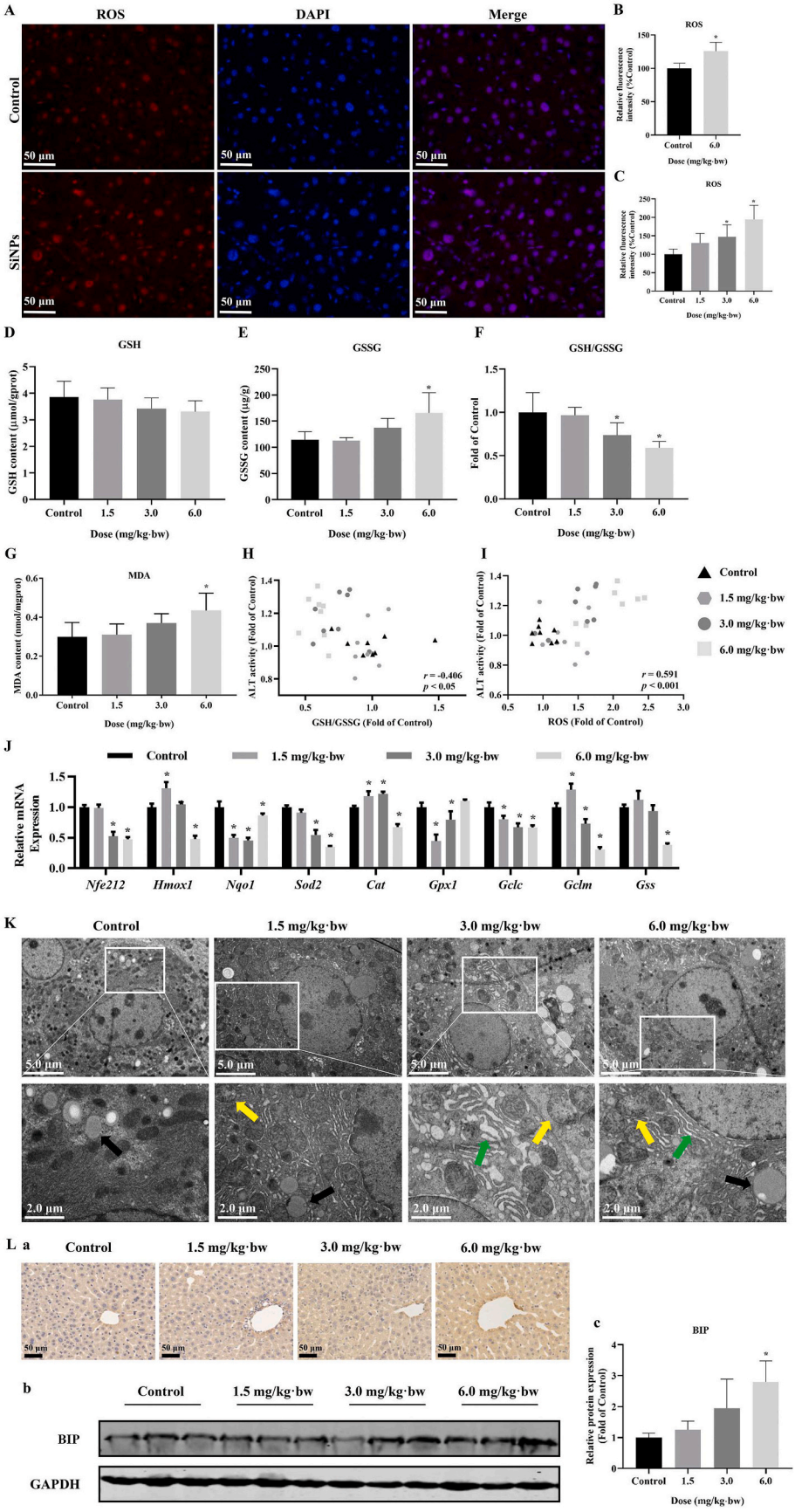

Fig. 4. Oxidative stress and ER stress induced by SiNPs in the liver. Representative images (A) and corresponding analysis (B) of ROS staining in liver (n = 3 per group), and also, the quantitative analysis of hepatic ROS content by FCM (C; n = 8 per group) were performed. The scale bar, 50 μm. According to the biochemical determination, declined GSH (D) and the ratio of GSH to GSSG (F), whilst increased GSSG (E) and MDA content (G) were induced by SiNPs (n = 8 per group). Meanwhile, hepatic ALT level was correlated with both GSH/GSSG (H) and ROS (I). (J) Relative mRNA expression of genes involved in Nrf2 signaling pathways (n = 4 per group). (K) Ultrastructure observation of mice liver by TEM. Mitochondrial deformation (yellow arrow), lipid droplets (black arrow), and swollen, fractured ER (green arrow) were seen. The scale bar, 2.0 or 5.0 μm. Immunohistochemical images of BIP (L-a), and BIP protein expression (L-b) and its analysis (L-c) in the liver. The scale bar, 50 μm (n = 3 per group). Data are shown as mean ± SD. *$p < 0.05$ *vs* control. (For interpretation of the references to color in this figure legend, the reader is referred to the Web version of this article.)

showed a significant down-regulation of Nrf2 signaling pathway caused by SiNPs (Fig. 4J). Noteworthy, the transcriptional up-regulation of some genes (*Hmox1*, *Cat*, *Gclm* and *Gss*) at a lower dose may due to a compensatory mechanism to maintain redox balance. Anyway, these results indicated SiNPs exposure triggered oxidative stress, leading to lipid peroxidation and resultant liver injury.

Apart from oxidative stress, the induction of ER stress was also detected in SiNPs-exposed liver tissues, as demonstrated by the ultrastructural observation (Fig. 4K) and enhanced hepatic BIP level (Fig. 4L). Upon SiNPs stimuli, hepatocytes manifested remarkable abnormalities in ER ultrastructure, ranging from spacing dilation, ribosome detachment to pronounced structural disruption: ER was swollen and fractured, and its coherence was broken (Fig. 4K). Besides, mitochondrial deformation including cristae rupture and disappearance, as well as larger amount of lipid droplet formation in the cytoplasm were observed in the SiNPs-treated liver tissues when compared to that of the control (Fig. 4K).

3.5. Metabolomic analysis revealing the metabolic response to SiNPs in the liver of HFD-fed ApoE$^{-/-}$ mice

Totally, 2238 positive and 820 negative ion peaks were obtained. The cluster of QC samples exhibited stability and repeatability of the metabolic analysis system (Fig. 5A). As the explanatory rate of model, R^2X and Q^2 are the main parameters for judging quality and predicting model, respectively. The following PCA score plot exhibited a clear grouping trend among the groups (Fig. 5B). Moreover, as shown in Fig. 5C and D, the samples of 3.0 or 6.0 mg/kg·bw group were significantly segregated from those in the control group, in despite of overfitting occurred in 1.5 mg/kg·bw when compared to the control. The details of three modes were shown in Supplementary files, Fig. S1.

Compared to the control, a total of 27 (3.0 mg/kg·bw) or 42 (6.0 mg/kg·bw) significantly changed metabolites (SCMs) were filtered out and identified based on VIP > 1.0 and $p < 0.05$ (FDR corrected) as shown in Fig. 5E. Specifically, 25 kinds of SCMs were identified in both 3.0 and

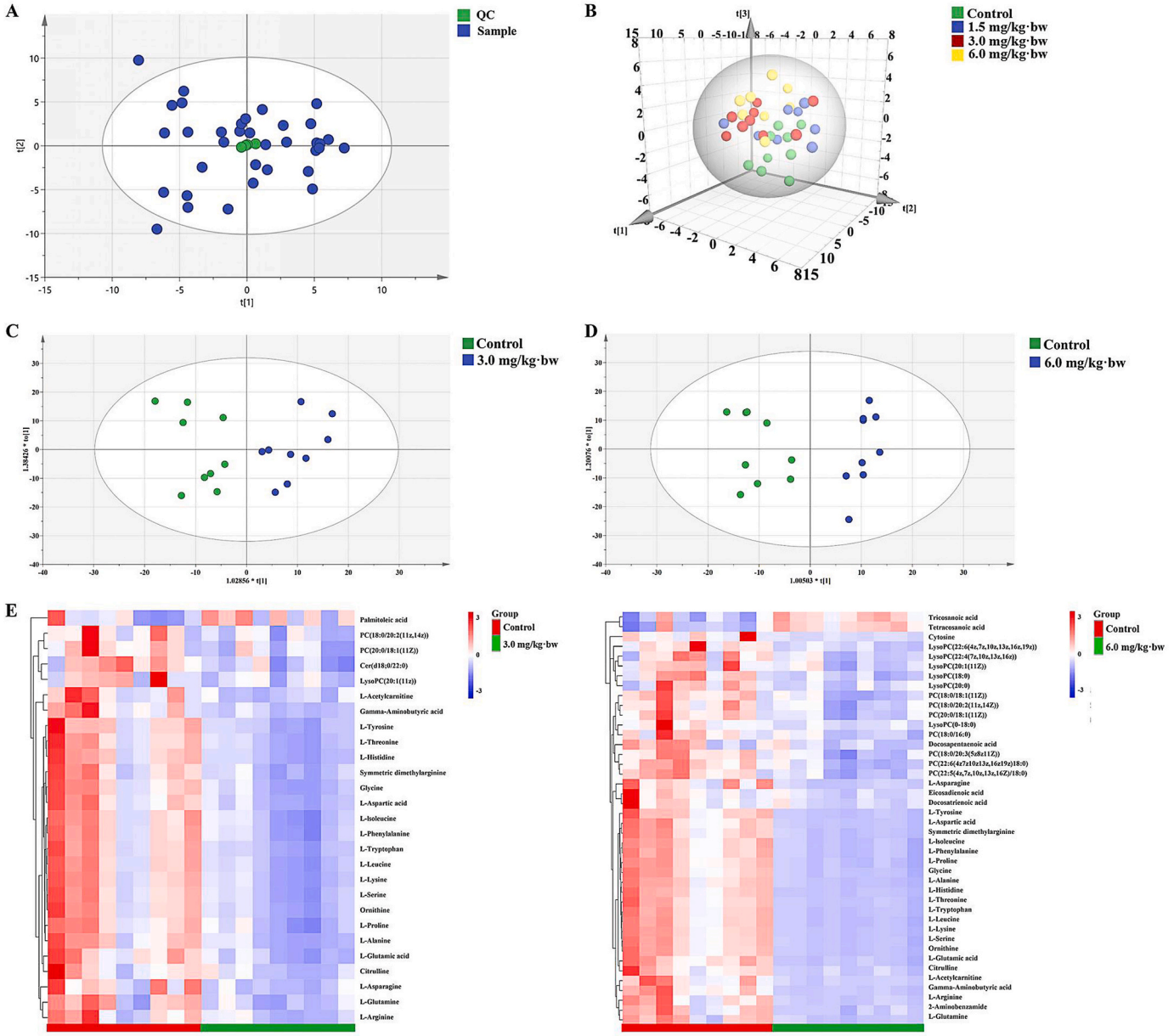

Fig. 5. Primary screening and related analysis of metabolites. (A) QC of reversed phase C_{18} separation. (B) The PCA scores plot, and OPLS-DA analysis of positive mode for RPC (C, D) were shown. n = 9 per group, except for 8 samples for 1.5 mg/kg·bw group. (E) Heatmap analysis for 3.0 and 6.0 mg/kg·bw SiNPs group, respectively. QC, quality control; RPC, reversed-phase chromatography.

6.0 mg/kg·bw groups, and manifested dose-dependent decline trend after SiNPs exposure, including 2 PC, 1 LysoPC, and 22 amino acids. See details in Supplementary Table S3.

3.6. SiNPs disturbed amino acid and lipid metabolisms, contributing to oxidative stress and lipid deposition in the HFD-fed ApoE$^{-/-}$ mice liver

Taking advantage of MetaboAnalyst 4.0 software, the SCMs-related potential pathways were analyzed. Interestingly, a series of amino acid metabolic pathways were dysregulated in mice liver, in particular, alanine, aspartate and glutamate metabolism, arginine and proline metabolism and glycine, serine and threonine metabolism as the top three pathways (Fig. 6A and B). Further metabolic pathway analysis as depicted in Fig. 6C showed, levels of SCMs involved in the top-three metabolism pathways were remarkably down-regulated by SiNPs in a dose-dependent manner. Besides, the potential signaling pathways with pathway impact greater than 0.1 were listed in Supplementary file, Table S4.

Interesting, the 27 of 44 kinds of SCMs were involved in the occurrence and development of liver-related diseases (Fig. 7A). A visible correlation network among these SCMs was calculated by using Cytoscape 3.6.1, suggesting that metabolic changes were not accidental, instead, SiNPs caused an alteration in entire metabolic network (Fig. 7B). Further, there was a clear statistical correlation between the oxidative stress-related indicators (including MDA, ROS and GSH/GSSG) and hepatic TC/TG levels (Fig. 7C), implying oxidative stress as a crucial player in lipid accumulation caused by SiNPs. Moreover, well correlations were also manifested between these identified SCMs (Fig. 7D). More importantly, the correlations between SCMs and above-mentioned indicators were analyzed (Fig. 7E). It is worth mentioning that the vast majority of SCMs were strongly correlated with the alterations in hepatic TC, TG, MDA, ROS and GSH/GSSG. These indicated SiNPs exacerbated metabolic-related oxidative injury in liver tissue, in particular, *via* amino acid- and lipid-related metabolism disorder, contributing to the lipid accumulation and hepatic steatosis in the progression of MAFLD.

4. Discussion

Increasing evidence suggested the development of MAFLD was highly dependent on the environment, especially with tremendous influence by toxicant exposure [38]. Liver is commonly regarded as a major organ for deposition of NPs after absorption. Previous studies have revealed SiNPs exposure could cause inflammation, liver injury and even hepatic fibrosis [7,39,40], hinting its possible role on the development of MAFLD. Indeed, our data revealed SiNPs exposure facilitated the progression of MAFLD using *in vivo* and *in vitro* investigations. In HFD-fed ApoE$^{-/-}$ mice model, the sub-chronic exposure to SiNPs greatly promoted lipid accumulation and even collagen deposition in the liver based on histopathological analysis and hepatic TC/TG quantification, resulting in greatly increased hepatic activities of ALT, AST and LDH (Fig. 2). Consistently, lipid accumulation was also enhanced by SiNPs in FFA-treated hepatocytes (Fig. 3). Among the patients with MAFLD, de novo lipogenesis (DNL) is considered to contribute about one-third of the TG stored in the liver. In the pathophysiology of fatty liver disease, TG accumulation is thought to exceed and hinder oxidative catabolism of FFA [41]. What's more, the increased fatty acid synthesis whilst inhibited fatty acid β-oxidation and lessened

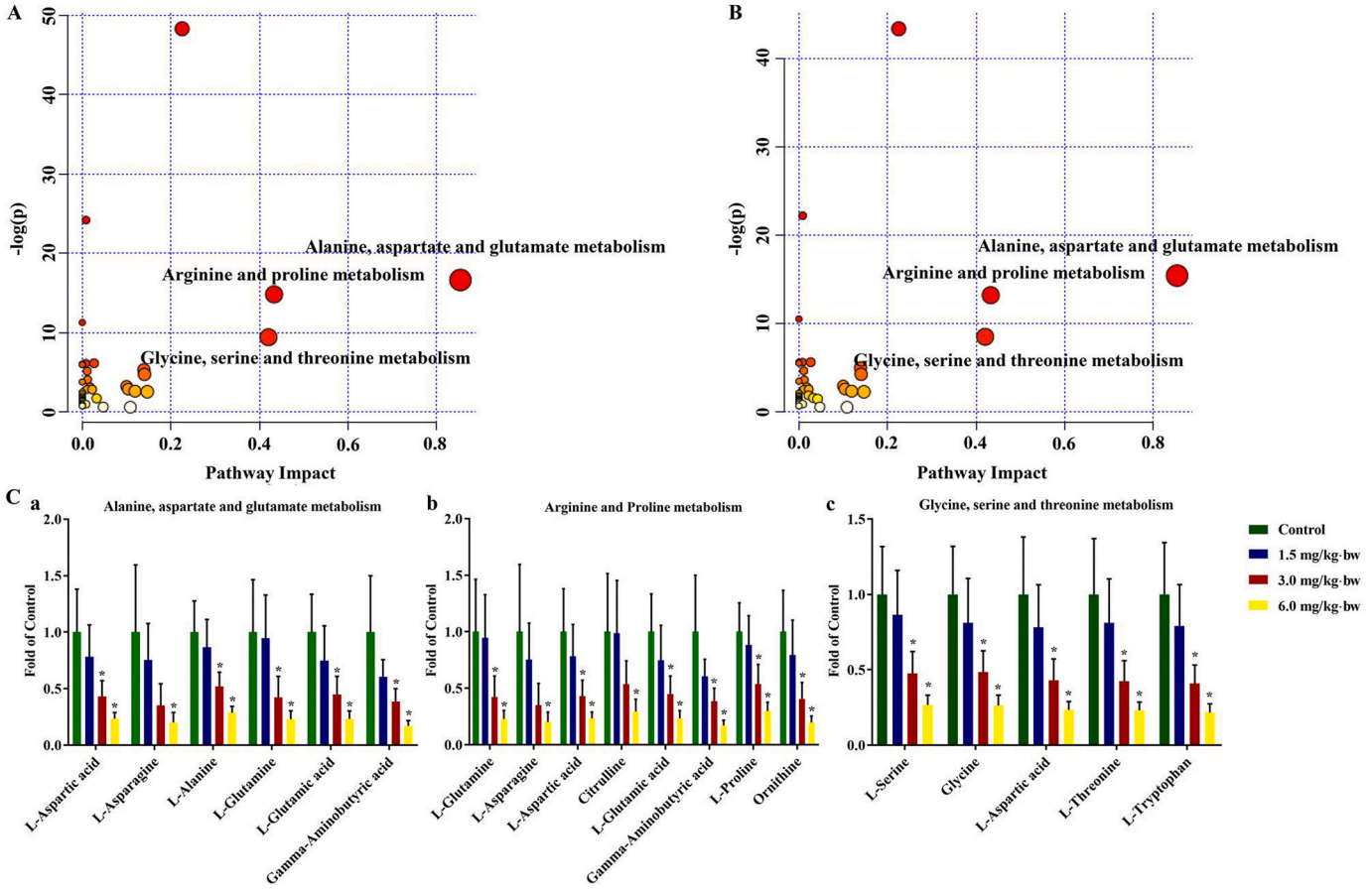

Fig. 6. MetPA analysis of identified metabolites. MetPA analysis for 3.0 (A) and 6.0 mg/kg·bw SiNPs group (B). (C) The relative expression of enriched metabolites in the first three important metabolic pathways, including alanine, aspartate and glutamate metabolism (a), arginine and proline metabolism (b), and glycine, serine and threonine metabolism (c). Data are shown as mean ± SD. *$p < 0.05$ *vs* control.

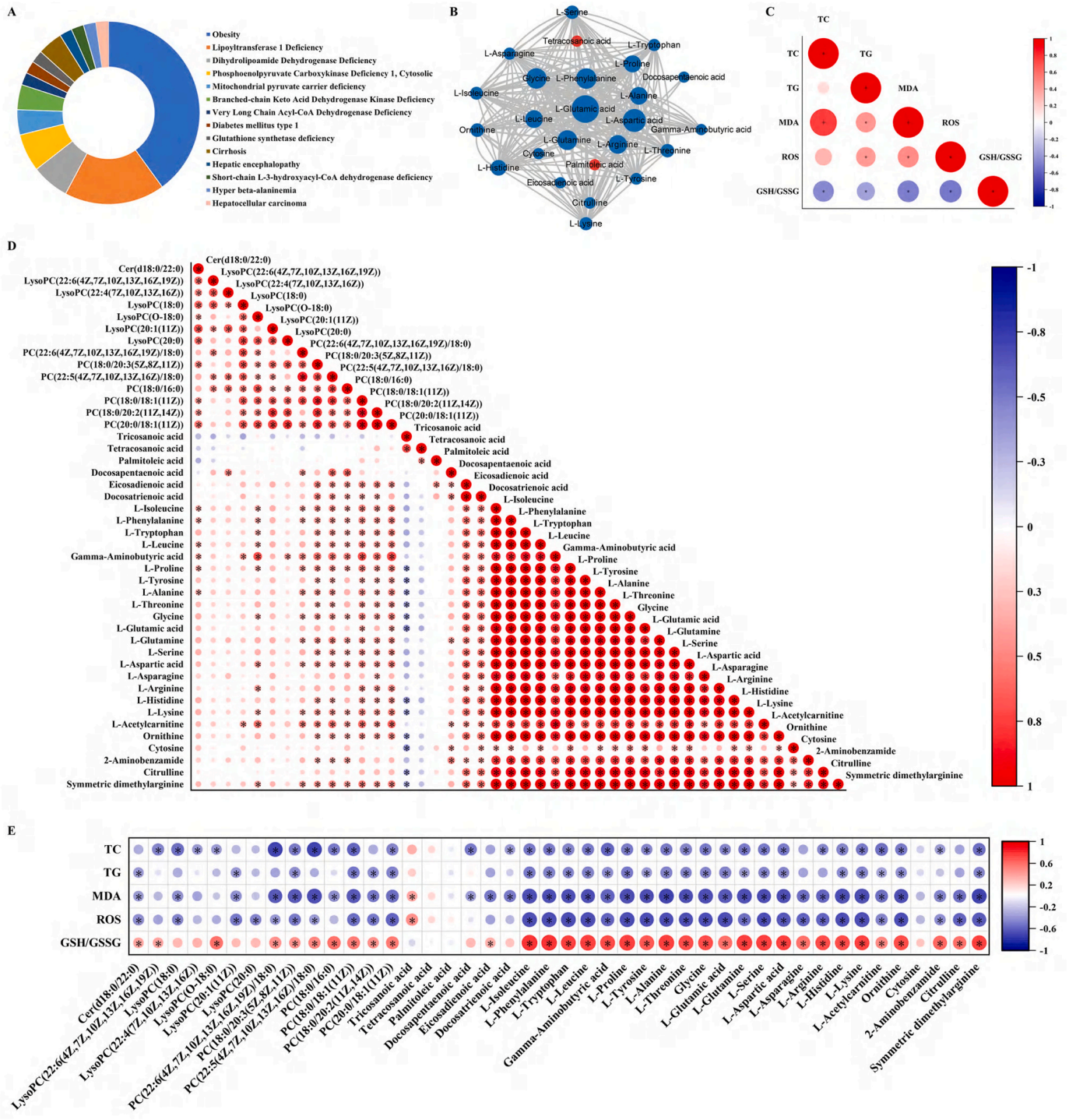

Fig. 7. The disturbed differential metabolites may contribute to the activation of oxidative stress and resultant hepatic steatosis, leading to liver-related diseases. These metabolites were associated with liver-related diseases (A). Altered metabolites were mapped to MetaboAnalyst and interaction network was generated in Cytoscape (B). Red and blue colors indicate up- and down-regulation of metabolite level, respectively. And area of the circle is correlated with the Betweeness centrality. Statistical correlations between oxidative stress- and hepatic steatosis-related indicators (C), between the identified differential metabolites (D), between metabolites and indicators (E) were analyzed. The deeper and larger the circle, the greater the correlation between the two indexes (n = 8 per group, $^*p < 0.05$). (For interpretation of the references to color in this figure legend, the reader is referred to the Web version of this article.)

lipid efflux contributed to the occurrence and progression of MAFLD, which was in line with our findings (Fig. 2K). Oppositely, MAFLD was improved by alleviating hepatic lipid accumulation and promoting fatty acid β-oxidation [42,43].

Inflammatory cytokines serve as significant roles in the development of MAFLD. For instance, the increased TNFα may play an important role in lipid metabolism and also hepatocyte death [44,45]. TNFα could promote cholesterol accumulation in hepatocytes by increasing intake through low-density lipoprotein (LDL) receptors and by inhibiting efflux through ABCG1. Lipid-accumulated hepatocytes are vulnerable to apoptosis or cell death in the presence of TNFα [46]. Concertedly, SiNPs promoted the expressions of *IL-6*, *IL-8* and *TNFα* in FFA-treated L02 cells

(Supplementary files, Fig. S2). Uysal *et al.* found that the expression levels of TNFα, IL-6 and IL-8 were significantly increased in patients with nonalcoholic steatohepatitis (NASH), which aggravated disease progression [47]. Oppositely, MAFLD was effectively alleviated in rats with type 2 diabetes mellitus (T2DM) by inhibiting inflammation [48].

Currently, metabolomics has been extensively applied to detect metabolic disorders and biomarkers in a variety of disease states [49]. When compared to histopathology and clinical chemistry, metabolomics exhibits improved sensitivity in identifying early events of toxicity [50]. Studies have found the perturbed metabolisms of amino acids, lipid, glucose, etc. were crucial to the fatty liver diseases [51,52]. ALT and AST may be sensors of global metabolic dysregulation. In the context of abnormally hepatic TG accumulation, the rise of aminotransferases was a consequence of the need to cope with liver metabolic derangement. Impressively, recent explorations on liver metabolism pointed out that rather than liver injury, elevated ALT and AST may be the consequence of impaired amino acid and energy metabolism in the liver [53]. In consideration of a dose-dependent hepatic lipid deposition and injury, the underlying mechanism involved was explored by UPLC-MS-based metabolomics analysis. As a result, SiNPs caused a global abnormal metabolism, as featured by disturbed PC, LysoPC, FFA, and amino acids as the potential differential metabolites. Of note, apart from the close associations among the identified differential metabolites, most of them were significantly correlated with hepatic TC and TG contents, and also the detected oxidative stress indicators (Fig. 7E). The findings highlighted the alterations of hepatic global metabolism as a key player in the progression of MAFLD upon SiNPs stimuli. Certainly, further in-depth exploration of the observed metabolites or pathway is of particular importance to fully elucidate the liver injury aggravated by SiNPs.

Notably, a majority of SCMs were amino acids, which was proposed as the more dominant regulator of hepatic metabolism. Liver is a critical organ for amino acid homeostasis, thereby confirming with our findings of declined levels of a series of amino acids in the SiNPs-administered liver and highlighting how disturbed amino acid metabolism can exacerbate hepatic injury. It is increasingly recognized that abnormality in amino acids could potentially impact energy metabolism, protein synthesis and proteolysis, fatty acid and urea synthesis, and cell signaling [54–57]. Increased evidence suggested a close link between imbalanced amino acid homeostasis and liver diseases. For instance, the intracellular TG level was found to be increased by amino acid deficiency without adding any lipid or hormones, and also low-amino acid diet facilitated the development of fatty liver [58]. Oppositely, the amino acid supply, such as citrulline [59], L-Carnitine [56], and L-Tryotophan [60], has been revealed to prevent the development of MAFLD in human and animal models, probably associated their anti-oxidant and anti-inflammation properties. Branched-chain amino acids could decrease plasma lipid levels and fat deposition in the liver [61]. Besides, glycine was also involved in purine biosynthesis and collagen synthesis within the liver [62], so it is therefore interesting to note that remarkable decreases in SiNPs-treated liver tissue, where we see advanced steatosis. In line with our findings, amnio acids, including glycine, alanine, aspartic acid, glutamic acid, and proline, were decreased in the liver of MAFLD rats induced by high-fat diet [63]. Besides, the dramatical reduction of glucogenic/ketogenic amino acids may attribute to a response to hepatic energy demands, and also reflect the promotion of gluconeogenesis as supported by the increased level of glycogen in SiNPs-treated liver through Periodic Acid-Schiff (PAS) staining (Supplementary files, Fig. S3). Interesting, a metabolomic study done by Lu *et al.* showed glucose among the significantly altered metabolites in liver tissue after SiNPs exposure [10].

Phospholipids are major structural components of cell membranes and plasma lipoprotein. The diminished phospholipids in liver caused by SiNPs may reflect a cascade of metabolic compensatory regulation for the plasma membrane re-synthesis, in order to resist the degradation of normal structural components [10]. Among these, PC was mainly synthesized by N-methylation reaction of PE in the liver [64]. Liver PC was closely associated with steatosis and essential for the regulation of TG biosynthesis and secretion [65]. It was unexpectedly revealed that the membrane lipid PC can be a precursor of ~65% TG in the liver. A declined PC content or insufficient synthesis of PC in liver was commonly accepted as an important factor to the formation of fatty liver. Puri *et al.* reported remarkable decline of hepatic PC and lipid subclasses in MAFLD patients, and alterations in PC metabolism were involved in MAFLD progression [66]. Walker *et al.* also found that blocking PC synthesis could increase lipid droplet accumulation [67]. In turn, a study provided evidence that PC supplement could execute hepatoprotective and anti-inflammatory functions in MAFLD mouse model through altering hepatic fatty acid composition [68]. Sphingolipid metabolism was also involved in a series of liver diseases [69]. Additionally, accumulated ceramides and altered LysoPCs have been implicated in the tissue impairment and dysfunction underlying metabolic disorders, including MAFLD [70]. Intriguingly, declined levels of one ceramide, Cer(d18:0/22:0), six LysoPC and seven types of PC were identified in SiNPs-treated liver tissue. Similarly, diminished LysoPC was detected by metabolomic analysis in mice models of alcoholic liver injury and liver cancer [71], and in high-fat diet induced obesity [72], especially LysoPC(16:0).

Increased levels of FFA in the liver is a sign of MAFLD, which are eventually converted to TG and stored as fat droplets, a process regarded as a protective mechanism for the liver to reduce toxic lipids. In contrast, the lipotoxicity of FFA and TG have been highlighted, *e.g.*, liver inflammation and cell death [73]. Exactly, the metabonomic analysis identified a marked accumulation of two saturated fatty acids (tricosanoic acid and tetracosanoic acid) and one monounsaturated fatty acid (palmitoleic acid) in SiNPs group, whilst dramatically declined three species of polyunsaturated fatty acids (docosapentaenoic acid, docosatrienoic acid and eicosadienoic acid). Unlike saturated fatty acids, polyunsaturated fatty acids were considered to be beneficial to health, and to execute some important physiologically functions, especially in the regulation of cholesterol/TG content and inflammatory response [74]. Meanwhile, ineffective disposal/storage of FFA can be a chronic source of ROS and could expedite lipid steatosis, inflammation and fibrosis in the development of MAFLD.

In agreement with our findings, the perturbations of arginine and proline metabolism, alanine, aspartate and glutamate metabolism and glycine, serine and threonine metabolism were also reported in hepatocellular injury/carcinoma [75]. The identified SCMs including glutamine, glutamic acid, asparagine, aspartic acid, alanine, citrulline, proline, ornithine, threonine, glycine, serine, tryptophan and γ-aminobutyric acid were involved in the disorder of these metabolic process in the progression of MAFLD upon SiNPs exposure. Similarly, declined glutamine, glycine, serine and proline, but increased phenylalanine was detected as the SCMs in the liver of 70 nm SiNPs-treated mice *via* intravenously injection [10]. Glutamine, glutamic acid and glycine are precursors of GSH, the liver's first line to defense against free radicals, and also inhibit inflammatory response and liver injury. Declined GSH was proposed as the potential biomarker of hepatocytes under oxidative stress stimuli [76]. Clinical study has demonstrated the reduced plasma glutamic acid acting as a biomarker for patients in early stages of septic shock with acute liver dysfunction [77]. The significant decreased levels of hepatic glutamine, glutamic acid and glycine highlighted the promotion of oxidative stress by SiNPs, as supported by the elevated ROS level in the liver or hepatocytes, as well as increased MDA content whilst declined GSH (Figs. 3 and 4). Importantly, in support of this notion, most of differential metabolites were strongly negative correlated to both hepatic ROS level and MDA content, whilst positive correlated to GSH/GSSG content in the liver (Fig. 7E). Similarly, an *in vitro* metabolomic analysis also claimed SiNPs suppressed glutathione metabolism and oxidative stress to trigger hepatoxicity [78]. Even worse, the accumulated cholesterol could consume the mitochondrial GSH, resulting in hepatic injury.

Oxidative stress was a key toxic mechanism involved in the adverse effects triggered by SiNPs [79–81]. Interestingly, oxidative stress was closely correlated with lipogenesis or lipolysis [82], and involved in pathological progression of MAFLD [83]. Ample evidence on the reversion of fatty liver by antioxidants therapy has provided powerful support for the contribution of oxidative stress to MAFLD [84]. Accordingly, the oxidative stress measurements *in vivo* (Fig. 4) and *in vitro* (Fig. 3) and corresponding correlation analysis (as depicted in Fig. 7C) have suggested SiNPs-elicited oxidative stress as a key contributor to hepatic lipid accumulation, resulting in the progression of MAFLD. In addition, we noted a down-regulated Nrf2 signaling in the liver of SiNPs group, a well-known intrinsic anti-oxidant pathway. Emerged evidence showed that the transcription factor Nrf2 also contributes to lipid homeostasis, other than anti-oxidant and anti-inflammatory stress [85]. And loss of Nrf2 enhanced the induction of lipogenic genes and reduced the expressions of beta-oxidation genes [86]. On the contrary, abnormal lipid metabolism can cause oxidative stress through nuclear receptors [87].

Studies have gradually revealed the roles of amino acids in oxidative stress and liver diseases. For example, L-Leucine could protect DNA damage from oxidative stress as a free radical scavenger [88], and reverse fat accumulation and metabolic disorder in Balb/c mice caused by cigarette [57]. Gamma aminobutyric acid (GABA) can reduce the oxidative stress and prevent obesity in C57BL/6 mice fed with HFD [89]. In rats, L-glutamine and L-Arginine were confirmed to reduce chemicals-induced hepatotoxicity through regulating GSH and lipid peroxidation [54,90]. Likewise, the contents of MDA and ROS in mouse hepatocytes could be decreased by glycine treatment [91]. Here, remarkable associations with oxidative stress-related indicators (i.e., ROS, GSH/GSSG, MDA) and also hepatic steatosis (TC and TG) were present in a majority of the identified SCMs (Fig. 7E). In this context, the detected perturbations by SiNPs from the metabolic perspective may account, at least in part, for the activation of oxidative stress and resultant hepatic steatosis.

Hepatocytes have highly developed ER, where the liver synthesizes fatty acids and metabolizes cholesterol. ER stress played a key role in the progression of hepatic steatosis, and proposed as the origin of a vicious pathological cycle in MAFLD [92]. Hepatic lipid overload could disturb ER function, leading to the activation of chronic ER stress, simultaneously, ER stress could promote lipid accumulation in hepatocytes, consequently causing or aggravating hepatic steatosis. ER stress has been suggested as an earlier biomarker for nanotoxicological evaluation [93]. We did confirm ER stress accompanied with mitochondrial dysfunction and oxidative stress, accounted for the toxic effects caused by SiNPs [94], including the emergency of perturbed lipid metabolism [32,95]. Given the ER structural abnormalities and increased BIP in the SiNPs-treated liver or hepatocytes (Figs. 3 and 4), the perturbations of lipid homeostasis were intrinsically linked with ER stress. Changes in the nutritional and energy states of the body can be sensed by ER [96]. When protein metabolism or membrane biogenesis/organization was suppressed, the hepatic ER function would shift from protein metabolism to lipid and carbohydrate metabolism [97]. That was in line with our metabolomic analysis. ER stress could promote hepatic DNL while inhibit hepatic fatty acid oxidation, contributing to the development of steatosis.

Given liver as one of the richest organs in terms of number and density of mitochondria, it is not surprising that mitochondrial dysfunction was likely to be a central player in the development of MAFLD [98]. Here, the ultrastructural observation also noticed the mitochondrial damage in the liver of mice after SiNPs administration (Fig. 4K). In line with this, SiNPs gradually impaired oxidative phosphorylation capacity and increased ROS level (Fig. 4A–C). Mitochondrion was confirmed as a key intracellular target for SiNPs [99,100,101], as well as a major source for ROS generation. Our *in vitro* study revealed the participation of mitochondrial dysfunction in hepatocytotoxicity caused by SiNPs [35]. Moreover, the disturbed mitochondrial quality control was responsible for particle-induced oxidative stress, mitochondrial dysfunction and the ultimate cell death [102,103,104]. In line with the disturbed amino acid-mediated oxidative stress induced by SiNPs in the liver, aspartic acid has been found to promote mitochondrial energy metabolism and prevent liver damage [50], as well as acylcarnitines being biomarkers for mitochondrial function [105,106]. Also, arginine could promote mitochondrial biosynthesis [107], and regulate lipid metabolism in mammals [108].

Importantly, a growing body of evidence pointed out the interplay among ER stress, oxidative stress and mitochondrial function. ER stress can arise owing to redox imbalance, and also reported to be responsible to the ROS generation and the induction of oxidative stress by SiNPs [109], ultimately contributing to inflammation, hepatic lipid accumulation and insulin resistance [110]. Collectively, these observations suggested SiNPs exposure promoted dysfunction of mitochondrion and ER in hepatocytes, thereby emerging chronic ER stress and oxidative stress that modulated lipid metabolism and resulted in progressive development of MAFLD. However, further functional studies are still in need to elucidate their specific roles in the SiNPs-induced progression of MAFLD, and to clarify the complex causal relationship between all these pathologic responses and ER/oxidative stress. What's more, it is still the focus of future research to alleviate oxidative damage and then mitigate MAFLD progress, probably through regulating metabolic strategy.

5. Conclusions

To our knowledge, this work firstly illuminated SiNPs led to the aggravation of MAFLD progression by using *in vivo* and *in vitro* models, mainly featured by the enhanced lipid accumulation and hepatic steatosis, as well as inflammatory response and even collagen deposition. The enhanced lipid deposition caused by SiNPs was associated with the promoted DNL whilst suppressed fatty acid β-oxidation and lipid efflux. More importantly, the metabolomic analysis revealed the disturbed amino acids and lipid metabolisms-mediated oxidative stress were the major contributors to hepatic injury aggravated by SiNPs. In general, our findings may be helpful to disclose the toxicity of SiNPs and offer a novel insight into the nanotoxicological investigation. The deleterious effects of SiNPs on humans, especially diseased individuals, shouldn't be ignored. Of note, the observed hepatotoxicity caused by SiNPs was dependent on the administered dosage, which would provide reference for SiNPs-related nanosafety assessment and exposure limit establishment.

Declaration of competing interest

All the authors have no conflict of interest.

Acknowledgements

This work was supported by National Natural Science Foundation of China (82273658, 82173551, 82073591).

Appendix A. Supplementary data

Supplementary data to this article can be found online at https://doi.org/10.1016/j.redox.2022.102569.

References

[1] Y. Yang, J. Li, Lipid, protein and poly(NIPAM) coated mesoporous silica nanoparticles for biomedical applications, Adv Colloid Interface Sci 207 (2014) 155–163.
[2] H.F. Krug, P. Wick, Nanotoxicology: an interdisciplinary challenge, Angew Chem Int Ed Engl 50 (6) (2011) 1260–1278.
[3] T. Kaewamatawong, A. Shimada, M. Okajima, H. Inoue, T. Morita, K. Inoue, H. Takano, Acute and subacute pulmonary toxicity of low dose of ultrafine colloidal silica particles in mice after intratracheal instillation, Toxicol Pathol 34 (7) (2006) 958–965.

[4] A. Nemmar, H. Vanbilloen, M.F. Hoylaerts, P.H. Hoet, A. Verbruggen, B. Nemery, Passage of intratracheally instilled ultrafine particles from the lung into the systemic circulation in hamster, Am J Respir Crit Care Med 164 (9) (2001) 1665–1668.

[5] W.G. Kreyling, M. Semmler-Behnke, J. Seitz, W. Scymczak, A. Wenk, P. Mayer, S. Takenaka, G. Oberdörster, Size dependence of the translocation of inhaled iridium and carbon nanoparticle aggregates from the lung of rats to the blood and secondary target organs, Inhal Toxicol 21 (Suppl 1) (2009) 55–60.

[6] S. Murugadoss, D. Lison, L. Godderis, S. Van Den Brule, J. Mast, F. Brassinne, N. Sebaihi, P.H. Hoet, Toxicology of silica nanoparticles: an update, Arch Toxicol 91 (9) (2017) 2967–3010.

[7] X. Li, Y. Li, S. Lv, H. Xu, R. Ma, Z. Sun, Y. Li, C. Guo, Long-term respiratory exposure to amorphous silica nanoparticles promoted systemic inflammation and progression of fibrosis in a susceptible mouse model, Chemosphere 300 (2022), 134633.

[8] Y.S. Kim, M.Y. Song, J.D. Park, K.S. Song, H.R. Ryu, Y.H. Chung, H.K. Chang, J. H. Lee, K.H. Oh, B.J. Kelman, I.K. Hwang, I.J. Yu, Subchronic oral toxicity of silver nanoparticles, Part Fibre Toxicol 7 (2010) 20.

[9] Y.N. Zhang, W. Poon, A.J. Tavares, I.D. McGilvray, W.C.W. Chan, Nanoparticle-liver interactions: cellular uptake and hepatobiliary elimination, J Control Release 240 (2016) 332–348.

[10] X. Lu, Y. Tian, Q. Zhao, T. Jin, S. Xiao, X. Fan, Integrated metabonomics analysis of the size-response relationship of silica nanoparticles-induced toxicity in mice, Nanotechnology 22 (5) (2011), 055101.

[11] A. Nemmar, P. Yuvaraju, S. Beegam, J. Yasin, E.E. Kazzam, B.H. Ali, Oxidative stress, inflammation, and DNA damage in multiple organs of mice acutely exposed to amorphous silica nanoparticles, Int J Nanomedicine 11 (2016) 919–928.

[12] Y. Zhu, Y. Zhang, Y. Li, C. Guo, Z. Fan, Y. Li, M. Yang, X. Zhou, Z. Sun, J. Wang, Integrative proteomics and metabolomics approach to elucidate metabolic dysfunction induced by silica nanoparticles in hepatocytes, J Hazard Mater 434 (2022), 128820.

[13] K. Isoda, E. Tetsuka, Y. Shimizu, K. Saitoh, I. Ishida, M. Tezuka, Liver injury induced by thirty- and fifty-nanometer-diameter silica nanoparticles, Biol Pharm Bull 36 (3) (2013) 370–375.

[14] S. Zhuravskii, G. Yukina, O. Kulikova, A. Panevin, V. Tomson, D. Korolev, M. Galagudza, Mast cell accumulation precedes tissue fibrosis induced by intravenously administered amorphous silica nanoparticles, Toxicol Mech Methods 26 (4) (2016) 260–269.

[15] A.M. Mahmoud, E.M. Desouky, W.G. Hozayen, M. Bin-Jumah, E.S. El-Nahass, H. A. Soliman, A.A. Farghali, Mesoporous silica nanoparticles trigger liver and kidney injury and fibrosis via altering TLR4/NF-κB, JAK2/STAT3 and Nrf2/HO-1 signaling in rats, Biomolecules 9 (10) (2019).

[16] J.V. Lafuente, A. Sharma, R. Patnaik, D.F. Muresanu, H.S. Sharma, Diabetes exacerbates nanoparticles induced brain pathology, CNS Neurol Disord Drug Targets 11 (1) (2012) 26–39.

[17] M. Eslam, A.J. Sanyal, J. George, MAFLD: a consensus-driven proposed nomenclature for metabolic associated fatty liver disease, Gastroenterology 158 (7) (2020) 1999–2014, e1991.

[18] G. Vernon, A. Baranova, Z.M. Younossi, Systematic review: the epidemiology and natural history of non-alcoholic fatty liver disease and non-alcoholic steatohepatitis in adults, Aliment Pharmacol Ther 34 (3) (2011) 274–285.

[19] Z.M. Younossi, A.B. Koenig, D. Abdelatif, Y. Fazel, L. Henry, M. Wymer, Global epidemiology of nonalcoholic fatty liver disease-Meta-analytic assessment of prevalence, incidence, and outcomes, Hepatology 64 (1) (2016) 73–84.

[20] B. Guo, Y. Guo, Q. Nima, Y. Feng, Z. Wang, R. Lu, Baimayangji, Y. Ma, J. Zhou, H. Xu, L. Chen, G. Chen, S. Li, H. Tong, X. Ding, X. Zhao, Exposure to air pollution is associated with an increased risk of metabolic dysfunction-associated fatty liver disease, J Hepatol 76 (3) (2022) 518–525.

[21] J. Heeren, L. Scheja, Metabolic-associated fatty liver disease and lipoprotein metabolism, Mol Metab 50 (2021), 101238.

[22] E.E. Powell, V.W. Wong, M. Rinella, Non-alcoholic fatty liver disease, Lancet 397 (10290) (2021) 2212–2224.

[23] C.H. Johnson, J. Ivanisevic, G. Siuzdak, Metabolomics: beyond biomarkers and towards mechanisms, Nat Rev Mol Cell Biol 17 (7) (2016) 451–459.

[24] D. Beyoğlu, J.R. Idle, Metabolomic and lipidomic biomarkers for premalignant liver disease diagnosis and therapy, Metabolites 10 (2) (2020).

[25] R.F. Dubin, E.P. Rhee, Proteomics and metabolomics in kidney disease, including insights into etiology, treatment, and prevention, Clin J Am Soc Nephrol 15 (3) (2020) 404–411.

[26] B. Zhang, M. Xie, L. Bruschweiler-Li, R. Brüschweiler, Nanoparticle-assisted metabolomics, Metabolites 8 (1) (2018).

[27] X. Zhao, A. Abulikemu, S. Lv, Y. Qi, J. Duan, J. Zhang, R. Chen, C. Guo, Y. Li, Z. Sun, Oxidative stress- and mitochondrial dysfunction-mediated cytotoxicity by silica nanoparticle in lung epithelial cells from metabolomic perspective, Chemosphere 275 (2021), 129969.

[28] M. Tous, N. Ferré, J. Camps, F. Riu, J. Joven, Feeding apolipoprotein E-knockout mice with cholesterol and fat enriched diets may be a model of non-alcoholic steatohepatitis, Mol Cell Biochem 268 (1-2) (2005) 53–58.

[29] N. Nasiri-Ansari, C. Nikolopoulou, K. Papoutsi, I. Kyrou, C.S. Mantzoros, G. Kyriakopoulos, A. Chatzigeorgiou, V. Kalotychou, M.S. Randeva, K. Chatha, K. Kontzoglou, G. Kaltsas, A.G. Papavassiliou, H.S. Randeva, E. Kassi, Empagliflozin attenuates non-alcoholic fatty liver disease (NAFLD) in high fat diet fed ApoE((-/-)) mice by activating autophagy and reducing ER stress and apoptosis, Int J Mol Sci 22 (2) (2021).

[30] C. Guo, Y. Xia, P. Niu, L. Jiang, J. Duan, Y. Yu, X. Zhou, Y. Li, Z. Sun, Silica nanoparticles induce oxidative stress, inflammation, and endothelial dysfunction in vitro via activation of the MAPK/Nrf2 pathway and nuclear factor-κB signaling, Int J Nanomedicine 10 (2015) 1463–1477.

[31] R. You, Y.S. Ho, C.H. Hung, Y. Liu, C.X. Huang, H.N. Chan, S.L. Ho, S.Y. Lui, H. W. Li, R.C. Chang, Silica nanoparticles induce neurodegeneration-like changes in behavior, neuropathology, and affect synapse through MAPK activation, Part Fibre Toxicol 15 (1) (2018) 28.

[32] R. Ma, Y. Qi, X. Zhao, X. Li, X. Sun, P. Niu, Y. Li, C. Guo, R. Chen, Z. Sun, Amorphous silica nanoparticles accelerated atherosclerotic lesion progression in ApoE(-/-) mice through endoplasmic reticulum stress-mediated CD36 up-regulation in macrophage, Part Fibre Toxicol 17 (1) (2020) 50.

[33] P. Bedossa, Utility and appropriateness of the fatty liver inhibition of progression (FLIP) algorithm and steatosis, activity, and fibrosis (SAF) score in the evaluation of biopsies of nonalcoholic fatty liver disease, Hepatology 60 (2) (2014) 565–575.

[34] J. Chen, J. Chen, H. Fu, Y. Li, L. Wang, S. Luo, H. Lu, Hypoxia exacerbates nonalcoholic fatty liver disease via the HIF-2α/PPARα pathway, Am J Physiol Endocrinol Metab 317 (4) (2019) E710–e722.

[35] Y. Qi, R. Ma, X. Li, S. Lv, X. Liu, A. Abulikemu, X. Zhao, Y. Li, C. Guo, Z. Sun, Disturbed mitochondrial quality control involved in hepatocytotoxicity induced by silica nanoparticles, Nanoscale 12 (24) (2020) 13034–13045.

[36] C. Guo, M. Yang, L. Jing, J. Wang, Y. Yu, Y. Li, J. Duan, X. Zhou, Y. Li, Z. Sun, Amorphous silica nanoparticles trigger vascular endothelial cell injury through apoptosis and autophagy via reactive oxygen species-mediated MAPK/Bcl-2 and PI3K/Akt/mTOR signaling, Int J Nanomedicine 11 (2016) 5257–5276.

[37] C. Guo, J. Wang, M. Yang, Y. Li, S. Cui, X. Zhou, Y. Li, Z. Sun, Amorphous silica nanoparticles induce malignant transformation and tumorigenesis of human lung epithelial cells via P53 signaling, Nanotoxicology 11 (9-10) (2017) 1176–1194.

[38] H. Wan, Y. Wang, H. Zhang, K. Zhang, Y. Chen, C. Chen, W. Zhang, F. Xia, N. Wang, Y. Lu, Chronic lead exposure induces fatty liver disease associated with the variations of gut microbiota, Ecotoxicol Environ Saf 232 (2022), 113257.

[39] J. Li, X. He, Y. Yang, M. Li, C. Xu, R. Yu, Risk assessment of silica nanoparticles on liver injury in metabolic syndrome mice induced by fructose, Sci Total Environ 628–629 (2018) 366–374.

[40] M. Sun, J. Zhang, S. Liang, Z. Du, J. Liu, Z. Sun, J. Duan, Metabolomic characteristics of hepatotoxicity in rats induced by silica nanoparticles, Ecotoxicol Environ Saf 208 (2021), 111496.

[41] A.L. Birkenfeld, G.I. Shulman, Nonalcoholic fatty liver disease, hepatic insulin resistance, and type 2 diabetes, Hepatology 59 (2) (2014) 713–723.

[42] Y. Liu, W. Xu, T. Zhai, J. You, Y. Chen, Silibinin ameliorates hepatic lipid accumulation and oxidative stress in mice with non-alcoholic steatohepatitis by regulating CFLAR-JNK pathway, Acta Pharm Sin B 9 (4) (2019) 745–757.

[43] O. Rom, Y. Liu, Z. Liu, Y. Zhao, J. Wu, A. Ghrayeb, L. Villacorta, Y. Fan, L. Chang, L. Wang, C. Liu, D. Yang, J. Song, J.C. Rech, Y. Guo, H. Wang, G. Zhao, W. Liang, Y. Koike, H. Lu, T. Koike, T. Hayek, S. Pennathur, C. Xi, B. Wen, D. Sun, M. T. Garcia-Barrio, M. Aviram, E. Gottlieb, I. Mor, W. Liu, J. Zhang, Y.E. Chen, Glycine-based treatment ameliorates NAFLD by modulating fatty acid oxidation, glutathione synthesis, and the gut microbiome, Sci Transl Med 12 (572) (2020).

[44] J. Henao-Mejia, E. Elinav, C. Jin, L. Hao, W.Z. Mehal, T. Strowig, C.A. Thaiss, A. L. Kau, S.C. Eisenbarth, M.J. Jurczak, J.P. Camporez, G.I. Shulman, J.I. Gordon, H.M. Hoffman, R.A. Flavell, Inflammasome-mediated dysbiosis regulates progression of NAFLD and obesity, Nature 482 (7384) (2012) 179–185.

[45] K. Miura, H. Ohnishi, Role of gut microbiota and Toll-like receptors in nonalcoholic fatty liver disease, World J Gastroenterol 20 (23) (2014) 7381–7391.

[46] W. Zhang, H. Kudo, K. Kawai, S. Fujisaka, I. Usui, T. Sugiyama, K. Tsukada, N. Chen, T. Takahara, Tumor necrosis factor-alpha accelerates apoptosis of steatotic hepatocytes from a murine model of non-alcoholic fatty liver disease, Biochem Biophys Res Commun 391 (4) (2010) 1731–1736.

[47] S. Uysal, F. Armutcu, T. Aydogan, K. Akin, M. Ikizek, M.R. Yigitoglu, Some inflammatory cytokine levels, iron metabolism and oxidan stress markers in subjects with nonalcoholic steatohepatitis, Clin Biochem 44 (17-18) (2011) 1375–1379.

[48] W. Zou, C. Zhang, X. Gu, X. Li, H. Zhu, Metformin in combination with malvidin prevents progression of non-alcoholic fatty liver disease via improving lipid and glucose metabolisms, and inhibiting inflammation in type 2 diabetes rats, Drug Des Devel Ther 15 (2021) 2565–2576.

[49] J.K. Nicholson, J.C. Lindon, Systems biology: metabonomics, Nature 455 (7216) (2008) 1054–1056.

[50] P. Mishra, Z. Gong, B.C. Kelly, Assessing biological effects of fluoxetine in developing zebrafish embryos using gas chromatography-mass spectrometry based metabolomics, Chemosphere 188 (2017) 157–167.

[51] P. Jegatheesan, S. Beutheu, G. Ventura, G. Sarfati, E. Nubret, N. Kapel, A. J. Waligora-Dupriet, I. Bergheim, L. Cynober, J.P. De-Bandt, Effect of specific amino acids on hepatic lipid metabolism in fructose-induced non-alcoholic fatty liver disease, Clin Nutr 35 (1) (2016) 175–182.

[52] L. Hodson, P.J. Gunn, The regulation of hepatic fatty acid synthesis and partitioning: the effect of nutritional state, Nat Rev Endocrinol 15 (12) (2019) 689–700.

[53] C.J. Pirola, S. Sookoian, Multiomics biomarkers for the prediction of nonalcoholic fatty liver disease severity, World J Gastroenterol 24 (15) (2018) 1601–1615.

[54] R.M. El-Sayed, H.I. Ahmed, A.E.S. Abd El-Lateef, A.A. Ali, Apoptosis perturbations and expression of regulatory inflammatory factors in cisplatin-depleted rat livers under l-arginine protection, Can J Physiol Pharmacol 97 (5) (2019) 359–369.

[55] T. Hanai, M. Shiraki, K. Imai, A. Suetugu, K. Takai, M. Shimizu, Usefulness of carnitine supplementation for the complications of liver cirrhosis, Nutrients 12 (7) (2020).

[56] D. Savic, L. Hodson, S. Neubauer, M. Pavlides, The importance of the fatty acid transporter L-carnitine in non-alcoholic fatty liver disease (NAFLD), Nutrients 12 (8) (2020).

[57] Y. Zeng, T. Huang, N. Wang, Y. Xu, C. Sun, M. Huang, C. Chen, B.G. Oliver, C. Yi, H. Chen, L-leucine improves metabolic disorders in mice with in-utero cigarette smoke exposure, Front Physiol 12 (2021), 700246.

[58] H. Nishi, D. Yamanaka, H. Kamei, Y. Goda, M. Kumano, Y. Toyoshima, A. Takenaka, M. Masuda, Y. Nakabayashi, R. Shioya, N. Kataoka, F. Hakuno, S. I. Takahashi, Importance of serum amino acid profile for induction of hepatic steatosis under protein malnutrition, Sci Rep 8 (1) (2018) 5461.

[59] W. Ouelaa, P. Jegatheesan, J. M'Bouyou-Boungou, C. Vicente, S. Nakib, E. Nubret, J.P. De Bandt, Citrulline decreases hepatic endotoxin-induced injury in fructose-induced non-alcoholic liver disease: an ex vivo study in the isolated perfused rat liver, Br J Nutr 117 (11) (2017) 1487–1494.

[60] H. Cichoz-Lach, K. Celinski, P.C. Konturek, S.J. Konturek, M. Slomka, The effects of L-tryptophan and melatonin on selected biochemical parameters in patients with steatohepatitis, J Physiol Pharmacol 61 (5) (2010) 577–580.

[61] T. Li, L. Geng, X. Chen, M. Miskowiec, X. Li, B. Dong, Branched-chain amino acids alleviate nonalcoholic steatohepatitis in rats, Appl Physiol Nutr Metab 38 (8) (2013) 836–843.

[62] Z. Schofield, M.A. Reed, P.N. Newsome, D.H. Adams, U.L. Günther, P.F. Lalor, Changes in human hepatic metabolism in steatosis and cirrhosis, World J Gastroenterol 23 (15) (2017) 2685–2695.

[63] Z. Xie, H. Li, K. Wang, J. Lin, Q. Wang, G. Zhao, W. Jia, Q. Zhang, Analysis of transcriptome and metabolome profiles alterations in fatty liver induced by high-fat diet in rat, Metabolism 59 (4) (2010) 554–560.

[64] A.B. Jordy, M.J. Kraakman, T. Gardner, E. Estevez, H.L. Kammoun, J.M. Weir, B. Kiens, P.J. Meikle, M.A. Febbraio, D.C. Henstridge, Analysis of the liver lipidome reveals insights into the protective effect of exercise on high-fat diet-induced hepatosteatosis in mice, Am J Physiol Endocrinol Metab 308 (9) (2015) E778–E791.

[65] J.N. van der Veen, S. Lingrell, D.E. Vance, The membrane lipid phosphatidylcholine is an unexpected source of triacylglycerol in the liver, J Biol Chem 287 (28) (2012) 23418–23426.

[66] P. Puri, R.A. Baillie, M.M. Wiest, F. Mirshahi, J. Choudhury, O. Cheung, C. Sargeant, M.J. Contos, A.J. Sanyal, A lipidomic analysis of nonalcoholic fatty liver disease, Hepatology 46 (4) (2007) 1081–1090.

[67] A.K. Walker, R.L. Jacobs, J.L. Watts, V. Rottiers, K. Jiang, D.M. Finnegan, T. Shioda, M. Hansen, F. Yang, L.J. Niebergall, D.E. Vance, M. Tzoneva, A.C. Hart, A.M. Näär, A conserved SREBP-1/phosphatidylcholine feedback circuit regulates lipogenesis in metazoans, Cell 147 (4) (2011) 840–852.

[68] A. Pathil, J. Mueller, A. Warth, W. Chamulitrat, W. Stremmel, Ursodeoxycholyl lysophosphatidylethanolamide improves steatosis and inflammation in murine models of nonalcoholic fatty liver disease, Hepatology 55 (5) (2012) 1369–1378.

[69] H. Nojima, C.M. Freeman, E. Gulbins, A.B. Lentsch, Sphingolipids in liver injury, repair and regeneration, Biol Chem 396 (6-7) (2015) 633–643.

[70] B. Chaurasia, S.A. Summers, Ceramides - lipotoxic inducers of metabolic disorders, Trends Endocrinol Metab 26 (10) (2015) 538–550.

[71] S. Li, H. Liu, Y. Jin, S. Lin, Z. Cai, Y. Jiang, Metabolomics study of alcohol-induced liver injury and hepatocellular carcinoma xenografts in mice, J Chromatogr B Analyt Technol Biomed Life Sci 879 (24) (2011) 2369–2375.

[72] S. Rai, S. Bhatnagar, Novel lipidomic biomarkers in hyperlipidemia and cardiovascular diseases: an integrative biology analysis, Omics 21 (3) (2017) 132–142.

[73] D.L. Gorden, D.S. Myers, P.T. Ivanova, E. Fahy, M.R. Maurya, S. Gupta, J. Min, N. J. Spann, J.G. McDonald, S.L. Kelly, J. Duan, M.C. Sullards, T.J. Leiker, R. M. Barkley, O. Quehenberger, A.M. Armando, S.B. Milne, T.P. Mathews, M. D. Armstrong, C. Li, W.V. Melvin, R.H. Clements, M.K. Washington, A. M. Mendonsa, J.L. Witztum, Z. Guan, C.K. Glass, R.C. Murphy, E.A. Dennis, A. H. Merrill Jr., D.W. Russell, S. Subramaniam, H.A. Brown, Biomarkers of NAFLD progression: a lipidomics approach to an epidemic, J Lipid Res 56 (3) (2015) 722–736.

[74] Y.H. Li, L.H. Yang, K.H. Sha, T.G. Liu, L.G. Zhang, X.X. Liu, Efficacy of poly-unsaturated fatty acid therapy on patients with nonalcoholic steatohepatitis, World J Gastroenterol 21 (22) (2015) 7008–7013.

[75] D. Cao, C. Cai, M. Ye, J. Gong, M. Wang, J. Li, J. Gong, Differential metabonomic profiles of primary hepatocellular carcinoma tumors from alcoholic liver disease, HBV-infected, and HCV-infected cirrhotic patients, Oncotarget 8 (32) (2017) 53313–53325.

[76] N. Wang, J. Wei, Y. Liu, D. Pei, Q. Hu, Y. Wang, D. Di, Discovery of biomarkers for oxidative stress based on cellular metabolomics, Biomarkers 21 (5) (2016) 449–457.

[77] M. Poeze, Y.C. Luiking, P. Breedveld, S. Manders, N.E. Deutz, Decreased plasma glutamate in early phases of septic shock with acute liver dysfunction is an independent predictor of survival, Clin Nutr 27 (4) (2008) 523–530.

[78] N. Chatterjee, J. Jeong, D. Yoon, S. Kim, J. Choi, Global metabolomics approach in in vitro and in vivo models reveals hepatic glutathione depletion induced by amorphous silica nanoparticles, Chem Biol Interact 293 (2018) 100–106.

[79] C. Guo, Y. Liu, Y. Li, Adverse effects of amorphous silica nanoparticles: focus on human cardiovascular health, J Hazard Mater 406 (2021), 124626.

[80] A. Abulikemu, X. Zhao, Y. Qi, Y. Liu, J. Wang, W. Zhou, H. Duan, Y. Li, Z. Sun, C. Guo, Lysosomal impairment-mediated autophagy dysfunction responsible for the vascular endothelial apoptosis caused by silica nanoparticle via ROS/PARP1/AIF signaling pathway, Environ Pollut 304 (2022), 119202.

[81] Y. Qi, H. Xu, X. Li, X. Zhao, Y. Li, X. Zhou, S. Chen, N. Shen, R. Chen, Y. Li, Z. Sun, C. Guo, Silica nanoparticles induce cardiac injury and dysfunction via ROS/Ca(2+)/CaMKII signaling, Sci Total Environ 837 (2022), 155733.

[82] Y.X. Pan, Z. Luo, M.Q. Zhuo, C.C. Wei, G.H. Chen, Y.F. Song, Oxidative stress and mitochondrial dysfunction mediated Cd-induced hepatic lipid accumulation in zebrafish Danio rerio, Aquat Toxicol 199 (2018) 12–20.

[83] E. Albano, E. Mottaran, G. Occhino, E. Reale, M. Vidali, Review article: role of oxidative stress in the progression of non-alcoholic steatosis, Aliment Pharmacol Ther 22 (Suppl 2) (2005) 71–73.

[84] A. Ferramosca, M. Di Giacomo, V. Zara, Antioxidant dietary approach in treatment of fatty liver: new insights and updates, World J Gastroenterol 23 (23) (2017) 4146–4157.

[85] E.H. Kobayashi, T. Suzuki, R. Funayama, T. Nagashima, M. Hayashi, H. Sekine, N. Tanaka, T. Moriguchi, H. Motohashi, K. Nakayama, M. Yamamoto, Nrf2 suppresses macrophage inflammatory response by blocking proinflammatory cytokine transcription, Nat Commun 7 (2016), 11624.

[86] P.J. Meakin, S. Chowdhry, R.S. Sharma, F.B. Ashford, S.V. Walsh, R. J. McCrimmon, A.T. Dinkova-Kostova, J.F. Dillon, J.D. Hayes, M.L. Ashford, Susceptibility of Nrf2-null mice to steatohepatitis and cirrhosis upon consumption of a high-fat diet is associated with oxidative stress, perturbation of the unfolded protein response, and disturbance in the expression of metabolic enzymes but not with insulin resistance, Mol Cell Biol 34 (17) (2014) 3305–3320.

[87] A. Ratneswaran, M.M. Sun, H. Dupuis, C. Sawyez, N. Borradaile, F. Beier, Nuclear receptors regulate lipid metabolism and oxidative stress markers in chondrocytes, J Mol Med (Berl) 95 (4) (2017) 431–444.

[88] O.L. Erukainure, O. Atolani, P. Banerjee, R. Abel, O.J. Pooe, O.S. Adeyemi, R. Preissner, C.I. Chukwuma, N.A. Koorbanally, M.S. Islam, Oxidative testicular injury: effect of L-leucine on redox, cholinergic and purinergic dysfunctions, and dysregulated metabolic pathways, Amino Acids 53 (3) (2021) 359–380.

[89] Z.X. Xie, S.F. Xia, Y. Qiao, Y.H. Shi, G.W. Le, Effect of GABA on oxidative stress in the skeletal muscles and plasma free amino acids in mice fed high-fat diet, J Anim Physiol Anim Nutr (Berl) 99 (3) (2015) 492–500.

[90] H. Türkez, F. Geyikoglu, M.I. Yousef, Modulatory effect of L-glutamine on 2,3,7,8 tetrachlorodibenzo-p-dioxin-induced liver injury in rats, Toxicol Ind Health 28 (7) (2012) 663–672.

[91] P.B. Pal, S. Pal, J. Das, P.C. Sil, Modulation of mercury-induced mitochondria-dependent apoptosis by glycine in hepatocytes, Amino Acids 42 (5) (2012) 1669–1683.

[92] A. Baiceanu, P. Mesdom, M. Lagouge, F. Foufelle, Endoplasmic reticulum proteostasis in hepatic steatosis, Nat Rev Endocrinol 12 (12) (2016) 710–722.

[93] R. Chen, L. Huo, X. Shi, R. Bai, Z. Zhang, Y. Zhao, Y. Chang, C. Chen, Endoplasmic reticulum stress induced by zinc oxide nanoparticles is an earlier biomarker for nanotoxicological evaluation, ACS Nano 8 (3) (2014) 2562–2574.

[94] C. Guo, R. Ma, X. Liu, Y. Xia, P. Niu, J. Ma, X. Zhou, Y. Li, Z. Sun, Silica nanoparticles induced endothelial apoptosis via endoplasmic reticulum stress-mitochondrial apoptotic signaling pathway, Chemosphere 210 (2018) 183–192.

[95] C. Guo, R. Ma, X. Liu, T. Chen, Y. Li, Y. Yu, J. Duan, X. Zhou, Y. Li, Z. Sun, Silica nanoparticles promote oxLDL-induced macrophage lipid accumulation and apoptosis via endoplasmic reticulum stress signaling, Sci Total Environ 631–632 (2018) 570–579.

[96] D.L. Eizirik, A.K. Cardozo, M. Cnop, The role for endoplasmic reticulum stress in diabetes mellitus, Endocr Rev 29 (1) (2008) 42–61.

[97] S. Fu, L. Yang, P. Li, O. Hofmann, L. Dicker, W. Hide, X. Lin, S.M. Watkins, A. R. Ivanov, G.S. Hotamisligil, Aberrant lipid metabolism disrupts calcium homeostasis causing liver endoplasmic reticulum stress in obesity, Nature 473 (7348) (2011) 528–531.

[98] M. Léveillé, J.L. Estall, Mitochondrial dysfunction in the transition from NASH to HCC, Metabolites 9 (10) (2019).

[99] C. Guo, J. Wang, L. Jing, R. Ma, X. Liu, L. Gao, L. Cao, J. Duan, X. Zhou, Y. Li, Z. Sun, Mitochondrial dysfunction, perturbations of mitochondrial dynamics and biogenesis involved in endothelial injury induced by silica nanoparticles, Environ Pollut 236 (2018) 926–936.

[100] X. Zhao, H. Xu, Y. Li, R. Ma, Y. Qi, M. Zhang, C. Guo, Z. Sun, Y. Li, Proteomic profiling reveals dysregulated mitochondrial complex subunits responsible for myocardial toxicity induced by SiNPs, Sci Total Environ 857 (Pt 1) (2022), 159206.

[101] X. Zhao, H. Xu, Y. Li, Y. Liu, X. Li, W. Zhou, J. Wang, C. Guo, Z. Sun, Y. Li, Silica nanoparticles perturbed mitochondrial dynamics and induced myocardial apoptosis via PKA-DRP1-mitochondrial fission signaling, Sci Total Environ (2022), 156854.

[102] X. Liu, X. Zhao, X. Li, S. Lv, R. Ma, Y. Qi, A. Abulikemu, H. Duan, C. Guo, Y. Li, Z. Sun, PM(2.5) triggered apoptosis in lung epithelial cells through the mitochondrial apoptotic way mediated by a ROS-DRP1-mitochondrial fission axis, J Hazard Mater 397 (2020), 122608.

[103] X. Zhao, H. Xu, X. Li, Y. Li, S. Lv, Y. Liu, C. Guo, Z. Sun, Y. Li, Myocardial toxicity induced by silica nanoparticles in a transcriptome profile, Nanoscale 14 (16) (2022) 6094–6108.

[104] Y. Li, Y. Zhu, B. Zhao, Q. Yao, H. Xu, S. Lv, J. Wang, Z. Sun, Y. Li, C. Guo, Amorphous silica nanoparticles caused lung injury through the induction of epithelial apoptosis via ROS/Ca^{2+}/DRP1-mediated mitochondrial fission signaling, Nanotoxicology (2022) 1–20, https://doi.org/10.1080/17435390.2022.2144774.

[105] C.R. Vissing, M. Dunø, F. Wibrand, M. Christensen, J. Vissing, Hydroxylated long-chain acylcarnitines are biomarkers of mitochondrial myopathy, J Clin Endocrinol Metab 104 (12) (2019) 5968–5976.
[106] S.M. Houten, R.J.A. Wanders, P. Ranea-Robles, Metabolic interactions between peroxisomes and mitochondria with a special focus on acylcarnitine metabolism, Biochim Biophys Acta Mol Basis Dis 1866 (5) (2020), 165720.
[107] W. Jobgen, C.J. Meininger, S.C. Jobgen, P. Li, M.J. Lee, S.B. Smith, T.E. Spencer, S.K. Fried, G. Wu, Dietary L-arginine supplementation reduces white fat gain and enhances skeletal muscle and brown fat masses in diet-induced obese rats, J Nutr 139 (2) (2009) 230–237.
[108] B. Tan, X. Li, Y. Yin, Z. Wu, C. Liu, C.D. Tekwe, G. Wu, Regulatory roles for L-arginine in reducing white adipose tissue, Front Biosci (Landmark Ed) 17 (6) (2012) 2237–2246.
[109] Y. Li, R. Ma, X. Liu, Y. Qi, A. Abulikemu, Endoplasmic reticulum stress-dependent oxidative stress mediated vascular injury induced by silica nanoparticles in vivo and in vitro - ScienceDirect, NanoImpact 14 (2019), 100169-100169.
[110] I. Hwang, M.J. Uddin, E.S. Pak, H. Kang, E.J. Jin, S. Jo, D. Kang, H. Lee, H. Ha, The impaired redox balance in peroxisomes of catalase knockout mice accelerates nonalcoholic fatty liver disease through endoplasmic reticulum stress, Free Radic Biol Med 148 (2020) 22–32.